International Journal of Multiphase Flow 36 (2010) 60–70

Contents lists available at ScienceDirect

International Journal of Multiphase Flow

journal homepage: www.elsevier.com/locate/ijmulflow

Nitrogen/non-Newtonian fluid two-phase upward flow in non-circular microchannels

Z.C. Yang, Q.C. Bi *, B. Liu, K.X. Huang

State Key Laboratory of Multiphase Flow in Power Engineering, Xi'an Jiaotong University, Xi'an, Shaanxi 710049, PR China

ARTICLE INFO

Article history:
Received 20 February 2009
Received in revised form 24 July 2009
Accepted 27 July 2009
Available online 31 August 2009

Keywords:
Non-Newtonian fluid
Two-phase flow pattern
Microchannel
Flow regime map

ABSTRACT

This paper presents experimental investigations on nitrogen/non-Newtonian fluid two-phase flow in vertical noncircular microchannels, which have square or triangular cross-section with the hydraulic diameters being D_h = 2.5, 2.886 and 0.866 mm, respectively, by visualization method. Three non-Newtonian aqueous solutions with typical rheological properties, i.e., 0.4% carboxymethyl cellulose (CMC), 0.2% polyacrylamide (PAM) and 0.2% xanthan gum (XG) are chosen as the working fluids. The common flow patterns are identified as slug flow, churn flow and annular flow. The dispersed bubble flow is only found in the case with nitrogen/CMC solution two-phase flow in the largest channel. A new flow pattern of nitrogen/PAM solution two-phase flow, named chained bubble/slug flow, is observed in all the test channels. The flow regime maps are also developed and the results show that the rheological properties of the non-Newtonian fluid have remarkable influence on the flow pattern transitions. The geometrical factors of the microchannel such as the cross-section shape and hydraulic diameter of the channel can also affect the flow regime map. Finally, the results obtained in this work are compared with the available flow pattern transitions.

1. Introduction

Gas/liquid two-phase flow is common in power engineering, chemical industry, petroleum refinery, process devices, and other related fields. Recently the emergence of the micro chemical technology demands high efficient reactors with more compact structure, which have to consider gas/non-Newtonian fluid two-phase flow in micro- or mini-channels. Since the morphology of two-phase flow always plays a critical role in determining the heat and mass transfer during the reaction process, it is essential to have a clear understanding of the physical mechanism of two-phase flow in micro- or mini-channels. A number of researches on two-phase flow patterns in small channel have been reported.

Triplett et al. (1999) conducted experimental investigations on air/water two-phase flow in circular microchannels with inner diameters of 1.1 and 1.45 mm, and in semi-triangular microchannels with hydraulic diameters of 1.09 and 1.49 mm, where the gas and liquid superficial velocity ranges from 0.02 to 80 and from 0.02 to 8 m/s, respectively. The discernible flow patterns were recognized as bubbly, churn, slug, slug-annular, annular, which occurred in all test sections. It shows that the flow pattern maps using gas and liquid superficial velocities as coordinates are similar. The results agree well with other experimental data and the inconsistencies can be attributed to the confusion in the identification of flow patterns. Comparison with available relevant regime transition models implies that there are generally poor agreements between the models and the experimental data.

Xu et al. (1999) carried out adiabatic air/water two-phase flow in vertical rectangular channels with narrow gaps of 0.3, 0.6 and 1.0 mm, respectively. It is observed that the flow regimes in channels with gaps of 1.0 and 0.6 mm are similar to those found in conventional larger channels. However, the flow regimes in the channel with the gap of 0.3 mm are dramatically different from previous studies; and the bubbly flow is not observed even at low gas flow rates. A new criterion has been developed to predict the transition of the annular flow.

Zhao and Bi (2001) performed an experimental study of co-current upward air/water two-phase flow in three vertical small triangular channels with hydraulic diameters of 2.886, 1.443 and 0.866 mm. The images of the two-phase flow patterns were taken by a high-speed motion analyzer and the flow regime maps for the three channels were developed. The results suggest that the typical flow patterns encountered in conventional, large-sized vertical circular tubes, such as dispersed bubbly flow, slug flow, churn flow and annular flow, can also be found in the two larger triangular channels while the dispersed bubbly flow is not found in the smallest triangular channel. A new type of flow patterns, referred as the capillary bubbly flow was identified, which is characterized by a single train of bubbles with ellipsoidal shape flowing upwards

* Corresponding author. Tel.: +86 29 82665287.
E-mail address: qcbi@mail.xjtu.edu.cn (Q.C. Bi).

0301-9322/$ - see front matter © 2009 Elsevier Ltd. All rights reserved.
doi:10.1016/j.ijmultiphaseflow.2009.07.011

along the channel axis. It is also found that in the slug flow regime, slug-bubbles are substantially elongated and the transition boundary from slug to churn and from churn to annular shift to the right as the hydraulic diameter of the triangular channels decrease according to the flow regime maps they obtained.

Hibiki and Mishima (2001) developed the flow-regime transition criteria for the vertical upward flow in narrow rectangular channels based on Mishima and Ishii model for round tubes. They compared the criteria with the existing experimental data for air–water flows in narrow rectangular channel with the gaps ranging from 0.3 to 17 mm and satisfactory agreements have been found. They concluded that a model for the gaps narrower than 1 mm should be modified in accordance with new flow regimes to be observed in a rectangular channel with a micro gap.

Serizawa et al. (2002) carried out visualized investigations on air–water two-phase flow in circular tubes with 20, 25 and 100 μm i.d. and steam–water flow in a 50 μm i.d. circular tube, with the superficial velocities covering a range $J_L = 0.003$–17.52 m/s and $J_G = 0.0012$–295.3 m/s. Some distinctive flow patterns and a special type of flow pattern were identified both in air–water and steam–water systems with their special features described. It concluded that two-phase flow patterns are sensitive to the surface conditions of the inner wall of the test tube. The comparison of the two-phase flow pattern map with the Mandhane's correlation (Mandhane et al., 1974) shows that general trends in the microchannels follow the Mandhane's prediction. And the cross-sectional average void fraction agrees well with the Armand correlation (Armand and Treschev, 1946) for larger tubes.

Kawahara et al. (2002) conducted experimental investigation of de-ionized water and nitrogen two-phase flow in a circular tube having diameter 100 μm, with superficial velocities of $J_G = 0.1$–60 m/s for gas, and $J_L = 0.02$–4 m/s for liquid. Two-phase flow patterns were recorded and a flow pattern map was developed based on the probability of appearance of each type of flow, and compared with the existing flow pattern maps obtained for 1-mm diameter channels.

Akbar et al. (2003) carried out gas–liquid two-phase flow experimental investigations in microchannels. They found that for $D_h \leqslant 1$ mm, the available data for near-circular microchannels and air–water like fluid pairs, are in reasonable agreement.

Saisorn and Wongwises (2008) studied air–water two-phase flow characteristics including flow pattern and two-phase friction pressure drop in a circular microchannel with a length of 320 mm, and an inner diameter of 0.53 mm. In their experiments, the superficial velocities of gas and liquid were in a range of 0.37–16 and 0.005–3.04 m/s, respectively. Slug flow, throat-annular flow, churn flow and annular-rivulet flow were observed and the flow pattern map was developed and compared with those by previous researchers. They attributed the discrepancies among the comparisons to the identification of flow pattern according to their definitions as well as the configurations of inlet and outlet sections.

The investigations mentioned above are all concerned with gas/Newtonian fluid two-phase flow in mini- or micro-channels. There are some studies focusing on gas/non-Newtonian fluid two-phase flow in channels as followed.

Dziubinski et al. (2004) developed a map of the rising flow of multi-phase mixtures of solid particles suspended in the non-Newtonian liquid and gas in vertical pipes with the inner diameters of 25.3, 40.6 and 50.5 mm, respectively. 5% water solutions of CMC and suspensions of 2–17.8 wt% spherical glass particles in CMC solutions were used as a continuous phase, which were treated as a homogeneous system. The same flow structures were observed during the flow of multi-phase mixtures with non-Newtonian liquids as those in the case of two-phase Newtonian liquid-gas flow. The results also suggest that the particles had no significant effect on the type of flow. They concluded that non-Newtonian features of liquids have negligible effect on the type of the two-phase flow structure and the most important appeared to be the apparent velocities of liquid and gas flow.

Cubaud et al. (2006) conducted experimental studies on two-phase flows in microchannels with surface modifications, i.e., hydrophilic and hydrophobic microchannels. The shapes of static and moving bubbles in microchannels with square cross-sections for different angles were investigated. The two-phase flows were made of pure water and air, and made of water with surfactant and air. The transient rheological behavior of polymer solutions was checked as the length of the polymers is comparable with the height of the channel. It is found that the measured viscosity of the solution is several times larger than the expected value and does not show typical shear-thinning behavior with polyacrylamide (PAM) solution being the working fluid.

Xu et al. (2007) conducted experimental investigations on co-current flow characteristics of air/non-Newtonian liquid system in inclined smooth tubes with diameters of 20, 40 and 60 mm. CMC solution was used as the non-Newtonian fluid. Bubbly flow, stratified flow, plug flow, slug flow, churn flow and annular flow were recognized. It is observed that the properties of non-Newtonian fluid have a minimal effect on the flow pattern in horizontal and near horizontal flow. It is also found that the non-Newtonian features of liquids exert a significant effect on void fraction of two-phase mixture flows, and the average void fraction decreases for specific J_G and J_L as the liquid becomes more shear-thinning.

For more detailed reviews on gas/liquid two-phase flow pattern may be found in Cheng et al. (2008). Based on the available research work on two-phase flow in mini- and micro-channels, it may be summarized that (i) the investigations on gas/Newtonian fluid two-phase flow in mini- and micro-channels have been conducted in depth and both circular and non-circular channel have been used; (ii) typical flow patterns for gas/Newtonian fluid have been identified and the flow regime maps have been presented. However, investigations on gas/Non-Newtonian fluid two-phase flow in non-circular mini- and micro-channels are still quite rare.

In this work, three typical non-Newtonian solutions are used as the working fluids. Visualized investigations on nitrogen/non-Newtonian two-phase flow in noncircular microchannels are performed. The typical images of the nitrogen/non-Newtonian two-phase flow pattern are recorded, and the corresponding flow regime maps are developed and discussed.

2. Experimental descriptions

2.1. Test loop

The experiments of nitrogen/non-Newtonian fluid two-phase flow in non-circular mini- and micro-channels are carried out in the test loop as sketched in Fig. 1. The whole test loop consists of two branches, i.e., the gas branch and the liquid branch. The high pressure nitrogen works not only as the part of the working fluid, but also as the impulse of the liquid flow. In the gas branch, the nitrogen is regulated by the controlled valve, and then is led through the needle valve and the flow-meter in turn before entering into the test section. Four thermal flow-meters (Cole-Parmer 32771 series) with different measuring ranges (50 ml/min, 500 ml/min, 5 L/min and 50 L/min) connected in parallel are used to determine the flow-rate of gas phase. A non-return valve is installed between the gas flow-meter and the test section in order to prevent the liquid phase from flowing into the gas branch. In the liquid branch, the high pressure nitrogen is led into the tank A to drive the liquid flow. The non-Newtonian liquid in tank A is

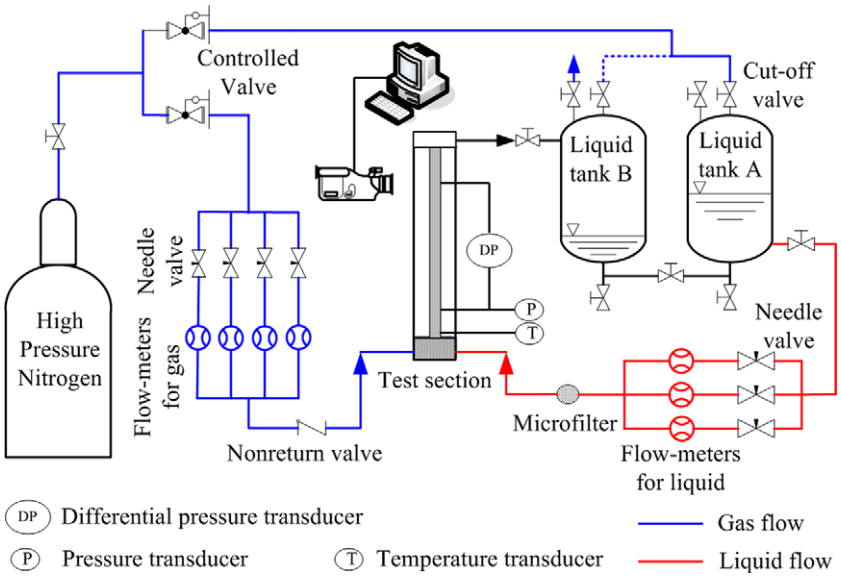

Fig. 1. Schematic of the nitrogen/non-Newtonian fluid two-phase flow test loop.

pushed through the needle valve, the flow-meter and the microfilter, and then enters the test section. The flow rate of the liquid phase is determined by three rotameters (LZB Series) connected in parallel with different ranges (16, 80 and 400 L/h).

A porous media is filled in the inlet plenum so that the gas and liquid phases can be mixed uniformly before flowing through the test area. The temperature of the two-phase mixture is determined by using a type K thermocouple. The local absolute pressure at the inlet of the test section and the pressure drop of two-phase flow are measured by two pressure transducers (Rosemont 3051 GP series) and the flow rate of the gas phase can be corrected according to the ideal gas equation of state.

During testing, the valve connecting the two tanks is shut off. Tank B works as a container for the exit liquid, of which two top valves are used with one cutting off from the high pressure nitrogen and the other open to the environment so that the nitrogen could exhaust to the atmosphere. When the working liquid in tank A is used up, the valve connecting the two tanks is opened for recharge. With tank B connected with high pressure nitrogen (see the dashed line in Fig. 1) and tank A open to the environment, the liquid in tank B can be pushed back into tank A by the high pressure. Hence, the working liquid can be reused during the experiments.

The data acquisition process is realized by IMP 3595 multichannel A/D board connected to an industry computer. The measured parameters are displayed in the screen of the computer synchronously to well monitor the experimental conditions. The data are stored for post-process and further analyses.

Visualization of the two-phase flow in microchannels is realized by using a high-definition camcorder (Sony DCR9000E) connected to the computer. The dynamic images of two-phase flow captured by the camcorder are displayed simultaneously on the screen of the computer and recorded in the hard disk. The camcorder can provide a wide shutter speed ranging from 1000 to 10,000 frames per minute. Hence, the flow patterns of the two-phase flow with gas superficial velocities $J_G = 0.1–100$ m/s and liquid superficial velocities $J_L = 0.01–6$ m/s can be identified distinctly.

The parameters measured in the test are the liquid flow rater, the gas flow rate, the absolute pressure at inlet and the two-phase pressure drop. It is estimated that the uncertainties of the liquid flow rate and the gas flow rate are ±2% and ±4.5%, respectively. The measured absolute pressure and pressure drop have a maximum error of 0.7% and 1.0%, respectively.

2.2. Test sections

The test channels used for nitrogen/non-Newtonian fluid two-phase flow in this work are schematically shown in Fig. 2, each having a non-circular cross-section (square or equilateral triangular). For convenience of flow visualization, the test sections are made of Lucite material by precision fabrication. The characteristic parameters of the test sections used in the present work are listed in Table 1. The channel dimensions are measured by a profile projector (Mitutoyo PJ311) and the maximum error is within ±3%.

2.3. Working fluids

Three typical non-Newtonian aqueous solutions are selected as the working fluids, namely, sodium carboxymethyl cellulose (CMC) with high viscosity and low elasticity, polyacrylamide (PAM) with low viscosity but high elasticity, xanthan gum (XG) whose rheological characteristics is somewhat like that of the blood. For convenience of comparison, the rheological characteristics of the non-Newtonian liquids are described in the form of power-law equation (Barnes, 2000), i.e.,

$$\tau = k(\dot{\gamma})^n \quad \text{and} \quad \mu = k(\dot{\gamma})^{n-1} \tag{1}$$

where τ is the shear stress, $\dot{\gamma}$ the shear rate, μ the dynamic viscosity; k is the fluid consistency coefficient and n the power-law index. The detailed physical and rheological parameters of the three working fluids are listed in Table 2 (Wu and Wu, 2002), where the zero shear viscosity, μ_0, and the infinite shear viscosity, μ_∞ are known as the apparent viscosity at very low and high shear rates, respectively. The relevant parameters of the water are also listed as the reference.

It can be noticed that the surface tension σ of the three solutions are close to that of water since the concentration of the solutions is relatively low.

3. Results and discussion

3.1. Nitrogen/CMC solution two-phase flow in microchannels

The images of typical two-phase flow patterns of nitrogen/CMC solution upward flow in non-circular microchannels are illustrated

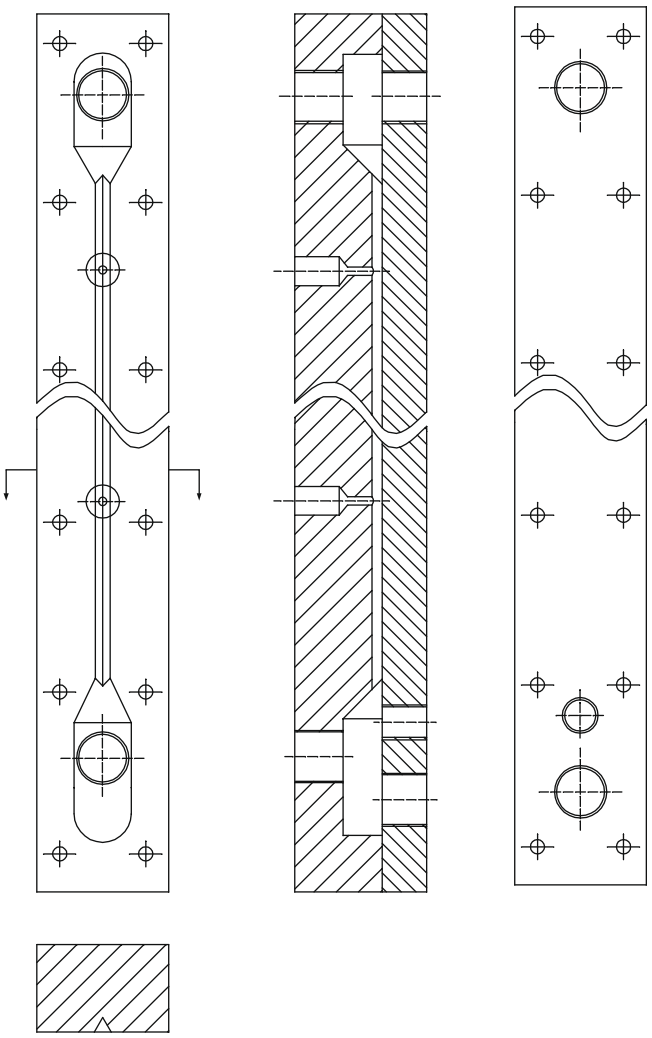

Fig. 2. Schematic structure of the test section.

Table 1
Parameters of the test section.

Section number	Cross-section	Side length, a (mm)	Hydraulic diameter, D_h (mm)	Test length, L (mm)
S1	Square	2.5	2.5	200
T2	Triangular	5	2.886	200
T3	Triangular	1.5	0.866	200

in Figs. 3–5, which are recorded at a shutter of 1/10,000 s. It is observed that the three typical flow patterns including slug flow (S), churn flow (C) and annular flow (A) in all the three channels, which are similar to the results of air/water two-phase flow previously reported by Zhao and Bi (2001).

Slug flow is observed when the gas superficial velocity is relatively low within the whole liquid superficial velocity range. It can be found from Figs. 3–5 that the gas slugs occupy most of the channel cross-section and are separated by the liquid plugs in the flow direction. When both liquid and gas superficial velocities are quite low, the gas slugs show a semi-ellipsoid shaped nose, a smooth body, and a semi-sphere shaped tail. As the gas superficial velocity goes up, the nose of the gas slugs gets an increased curvature, the body of the gas slugs elongates, and the tail of the gas slugs flattens. As the gas superficial velocity keeps increasing, the deformation of the gas slugs may get intensified and the slug tail cannot keep flat any more and gets disturbed, thus leading to churn flow.

As shown from Figs. 3–5, a churn flow occurs at moderate gas superficial velocities within the entire liquid superficial velocity range. In churn flow, the two-phase flow structure is extremely chaotic. The gas/liquid two-phase interface alters spatially and temporally without regular shapes.

When the gas superficial velocity is sufficiently high, an annular flow appears as characterized by a continuous gas core as well as a liquid film formed at the sidewalls of the channel. The gas core occupies almost the whole channel cross-section, and part of the liquid remains in the corner area of the channel. It is observed that there are fluctuations in the gas/liquid interface in the annular flow. As the gas superficial velocity increases, the amplitude of the fluctuation decreases but the frequency increases, as shown in Fig. 5.

Another flow pattern, the dispersed bubbly flow (DB) characterized by the presence of a cluster of small gas bubbles scattering in the continuous liquid phase, is observed to appear in the case with a high liquid velocity and low gas superficial velocity in the triangular channel T2 (see Fig. 4). It is noticed that the scattered gas bubbles takes on irregular shapes due to the fact that there is a high liquid velocity so that the bubbles are entrained dramatically by the liquid phase. However, the dispersed bubbly flow is not found in the smaller square channel with D_h = 2.5 mm (S1) and triangular channel with D_h = 0.866 mm (T3).

The flow regime maps of nitrogen/CMC solution two-phase upward flow in the microchannels are depicted in Fig. 6, in which various flow patterns are plotted using different symbols and the flow pattern transition lines are also marked.

According to the flow regime maps shown in Fig. 6, three flow patterns, namely, slug flow, churn flow and annular flow, are observed in the nitrogen/CMC solution two-phase flow in the present microchannels. It is noticed that dispersed bubble flow is observed in the larger triangular channel (T2, D_h = 2.886 mm), but not found in the other two channels with smaller hydraulic diameter (S1, D_h = 2.5 mm and S3, D_h = 0.866 mm). This trend is somewhat similar to the results of air–water co-current two-phase flow in microchannels by Zhao and Bi (2001). However, the capillary bubbly flow has not been found for nitrogen/CMC solution two-phase flow in the same triangular microchannel (D_h = 0.866 mm).

3.2. Nitrogen/PAM solution two-phase flow in microchannels

The flow pattern images of nitrogen/PAM solution two-phase in microchannels are exhibited in Figs. 7 and 8. Three typical flow patterns for nitrogen/PAM solution two-phase flow are identified

Table 2
Properties of the working fluids (22 °C).

Fluids	Molecular formula	Molecular weight	Concentration (wt%)	Surface tension, σ (N/m)	Rheological parameters		Apparent viscosity (mPa s)	
					k	n	μ_0	μ_∞
CMC	$(NaC_8H_{11}O_7)_m$	2.5×10^5–9×10^5	0.4	0.07152	0.372	0.7296	400	15
PAM	$(CH_2CHCONH_2)_m$	$\geqslant 3 \times 10^6$	0.2	0.07286	0.068	0.677	150	12
XG	$(C_{35}H_{49}O_{29})_m$	2×10^6–1.2×10^7	0.2	0.07335	0.1685	0.523	800	6.6
Water	H_2O	18	–	0.07269	1.004	1.0	1.004	–

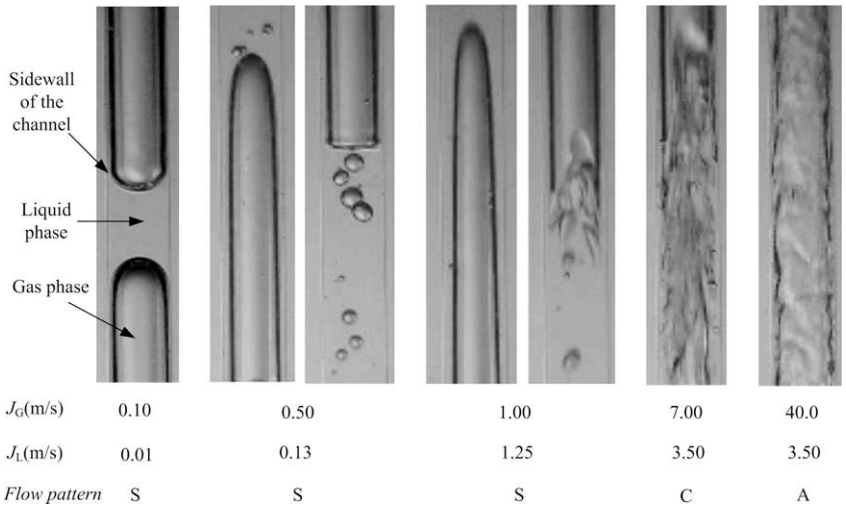

Fig. 3. Typical flow patterns of nitrogen/CMC solution in square channel (S1, D_h = 2.5 mm).

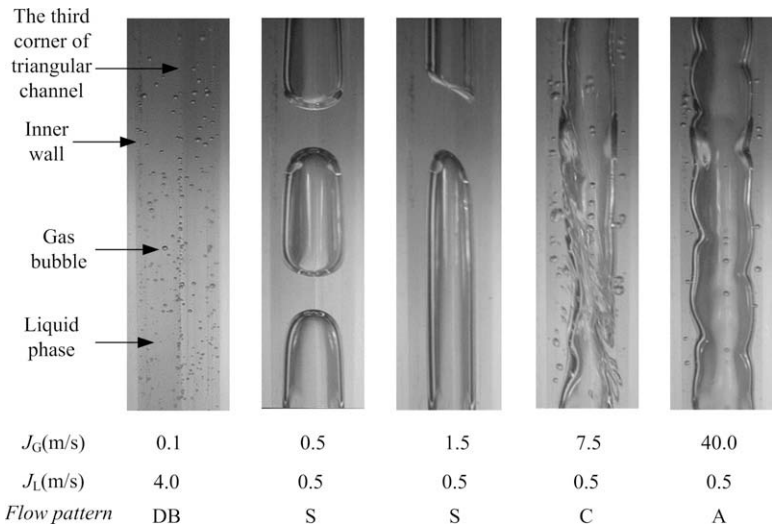

Fig. 4. Typical flow patterns of nitrogen/CMC solution in triangular channel (T2, D_h = 2.886 mm).

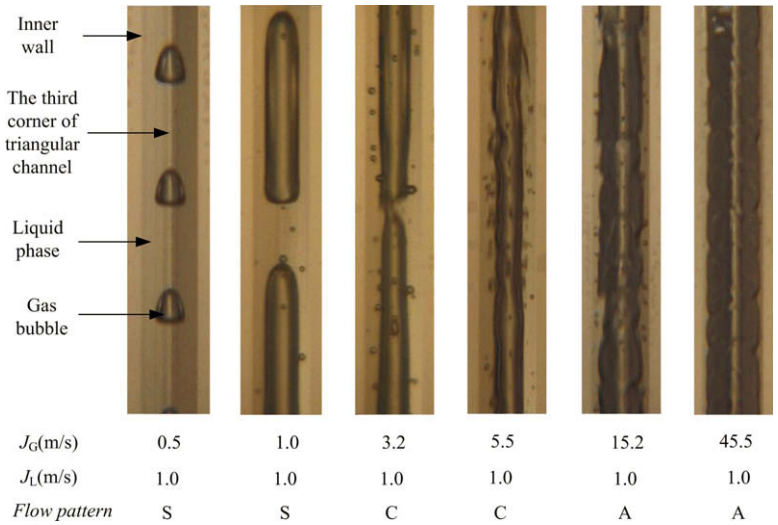

Fig. 5. Typical flow patterns of nitrogen/CMC solution in triangular channel (T3, D_h = 0.866 mm).

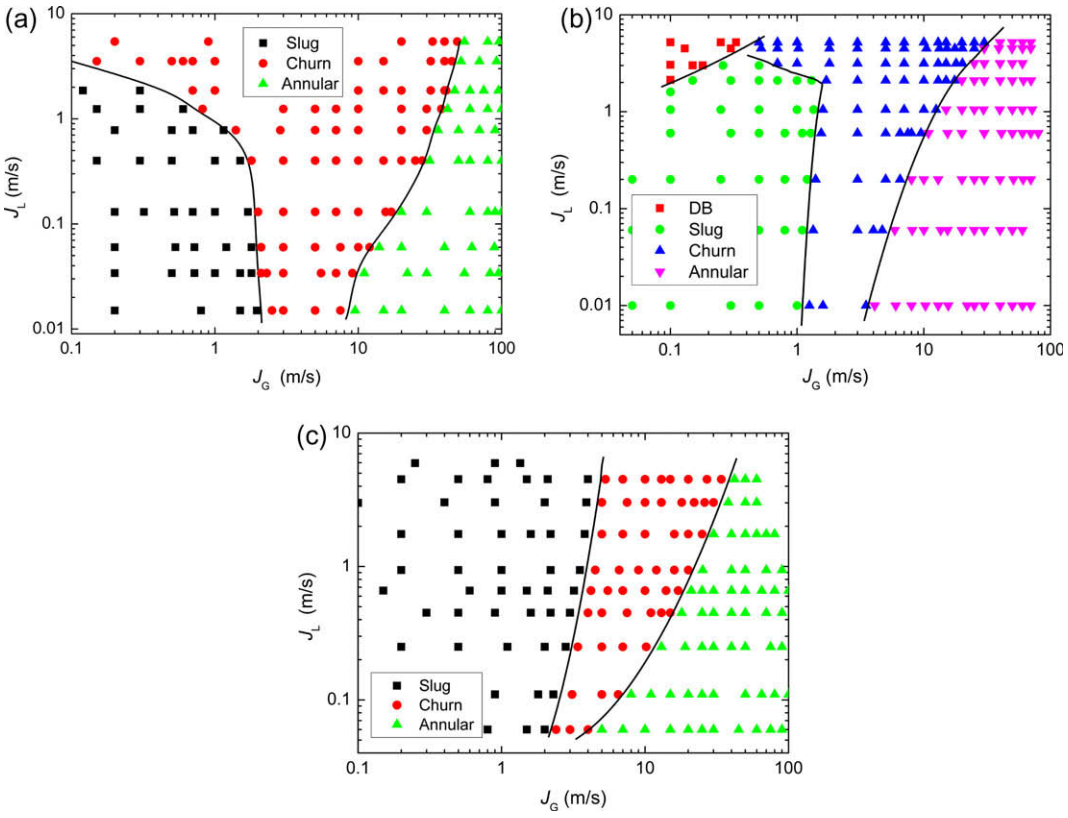

Fig. 6. Flow regime map of nitrogen/CMC solution two-phase upward flow in microchannels: (a) squared channel, D_h = 2.5 mm; (b) triangular channel, D_h = 2.886 mm; (c) Triangular channel, D_h = 0.866 mm.

in the present study, i.e., slug flow, churn flow and annular flow, which are similar to those found in nitrogen/CMC solution upward two-phase flow in microchannels. However, the detailed features of the flow patterns may be different.

A new flow pattern, named by chained bubble–slug (CBS) flow, is found in nitrogen/PAM solution two-phase flow in the microchannels, which is characterized by a chain of bubbles and small slugs flow in the center of the channel at low gas superficial velocity and moderate to high liquid superficial velocity. It is observed in the CBS flow the bubbles/slugs connected end to end but with apparent interface in between, especially when the liquid superficial velocity is relatively high (see Fig. 7). This flow pattern is quite different from the so-called bubble–train slug flow pattern in water–air two-phase (Chen et al., 2002). In the CBS flow, the dimensions of the bubbles and slugs observed is significantly smaller than the hydraulic diameter of the channel while the bubble and slugs in the bubble–train slug flow nearly occupy the whole cross-section of the channel with the dimensions equal to the hydraulic diameter of the channel.

It should be noted that the CBS flow is only observed in nitrogen/PAM solution two-phase flow and is not found in the other two nitrogen/non-Newtonian fluids two-phase flow. This appar-

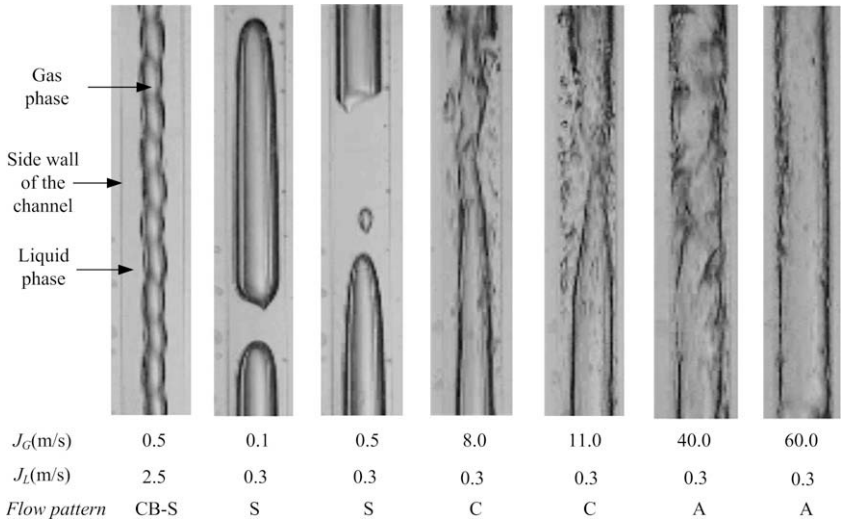

Fig. 7. Typical flow patterns of nitrogen/PAM two-phase flow in test section S1, D_h = 2.5 mm.

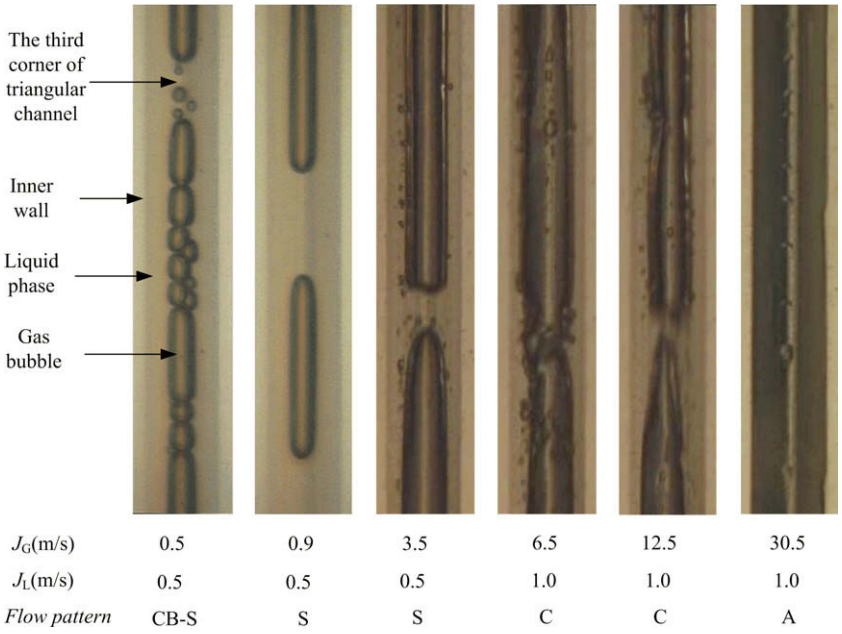

Fig. 8. Flow patterns of nitrogen/PAM solution two-channel in section T3, D_h = 0.866 mm.

ently indicates that the CBS flow should be caused by the peculiar rheological properties of the PAM solution. However, due to the complexity of the rheological characteristics of PAM solution, such as, microstructure of the solution, viscoelasticity, etc., it need further work to exactly explain the cause of the CBS flow pattern in nitrogen/PAM solution two-phase flow.

Fig. 9 illustrates the flow regime map of nitrogen/PAM solution in test section S1, D_h = 2.5 mm. It shows that in the cases with low liquid/gas superficial velocities, the slug flow appears while in the cases with high liquid superficial velocity and low gas superficial velocity, the CBS flow emerges. As the gas superficial velocity increases, the slug flow and annular flow take place in turn.

3.3. Nitrogen/XG solution two-phase flow in microchannels

Fig. 10 illustrates some typical two-phase flow patterns of nitrogen/XG solution in test section S1, namely, slug flow, churn flow, and annular flow. The same flow patterns are also observed in test section T2 and T3. When both superficial velocities of gas and liquid are relatively low, the stable gas slugs with hemispherical nose and smooth body take place. As the superficial velocities increases, the nose of the slug becomes sharper and the body of the slug becomes a bit distorted. When the superficial velocities increases further, the slugs will be broken into pieces dramatically and the churn flow occurs. There is no dispersed bubbly flow observed for nitrogen/XG two-phase flow in the present work.

Fig. 11 illustrates the flow regime map of nitrogen/XG in the microchannel (S1, D_h = 2.5 mm). It is found that the flow patterns of nitrogen/XG solution are similar to those of nitrogen/CMC in the same channel; however the transition conditions are apparently different from each other.

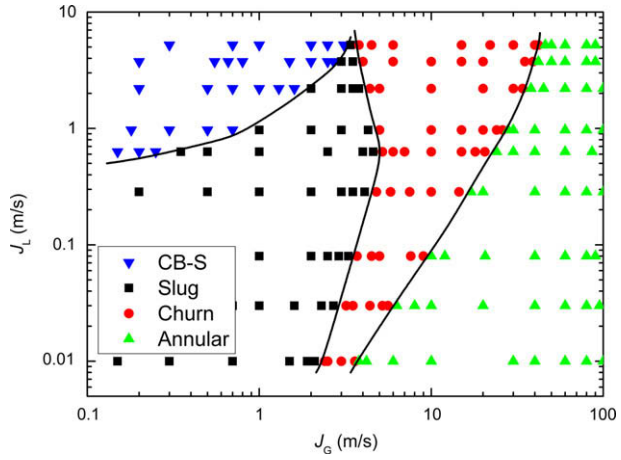

Fig. 9. Flow regime map of nitrogen/PAM solution two-phase flow in test section S1, D_h = 2.5 mm.

3.4. Comparison of the flow regime maps with different non-Newtonian liquids

In order to evaluate the viscous effect of the non-Newtonian fluids on the two-phase flow pattern transition, the effective viscosity is introduced here according to Spisak (1986)

$$\mu_{eff} = k\left(\frac{8J_L}{D_h}\right)^{n-1} \quad (2)$$

where k is the fluid consistency coefficient as listed in Table 2 and J_L is the superficial velocity of the liquid phase.

For the three non-Newtonian fluids used in the present work with the superficial liquid velocity ranges from 0.01 to 8.0 m/s, the effective viscosities are plotted in Fig. 12. It can be noticed from Fig. 12 that the effective viscosity of 0.4% CMC solution is much larger than those of the other two non-Newtonian solutions.

Fig. 13 exhibits the flow regime maps of those non-Newtonian liquids in the test section S1. It is observed that the churn flow region of nitrogen/CMC two-phase flow is much wider than those of the other two solutions. The reason may be due to the fact that the interaction between the gas and liquid phases becomes stronger when the effective viscosity is larger. This leads to earlier transition from slug flow to churn flow but later transition from slug flow to annular flow as the gas superficial velocity increases. However, the flow transition is not simply dependent of the effective viscosity of non-Newtonian fluids. For the 0.2% PAM solution and 0.2% XG solu-

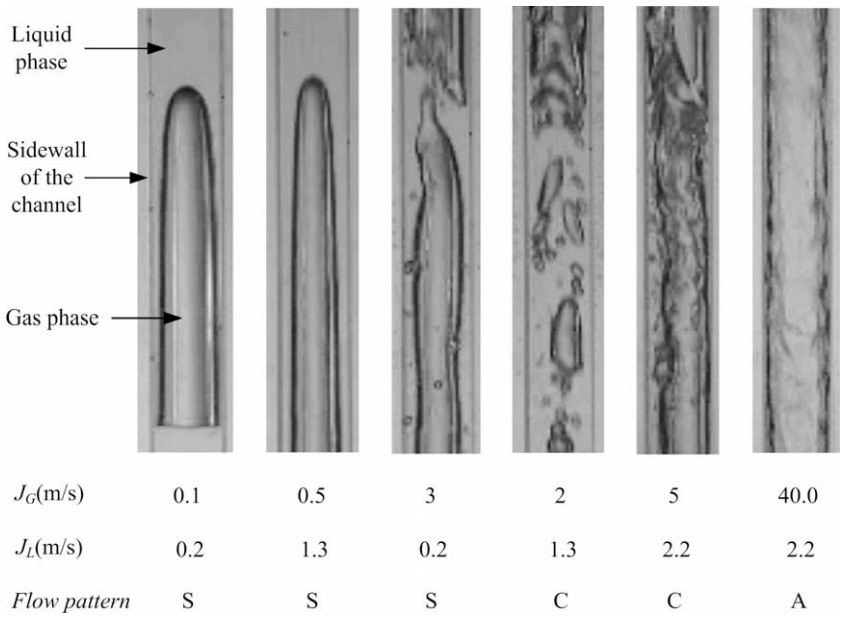

Fig. 10. Typical flow patterns of nitrogen/XG in the test section S1, D_h = 2.5 mm.

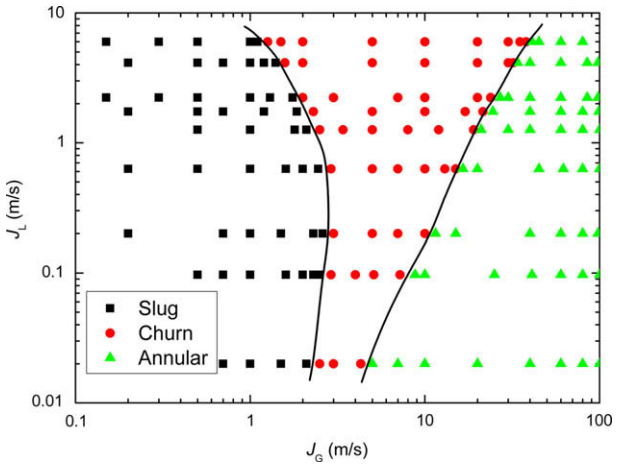

Fig. 11. Flow regime map of nitrogen/XG solution in test section S1, D_h = 2.5 mm.

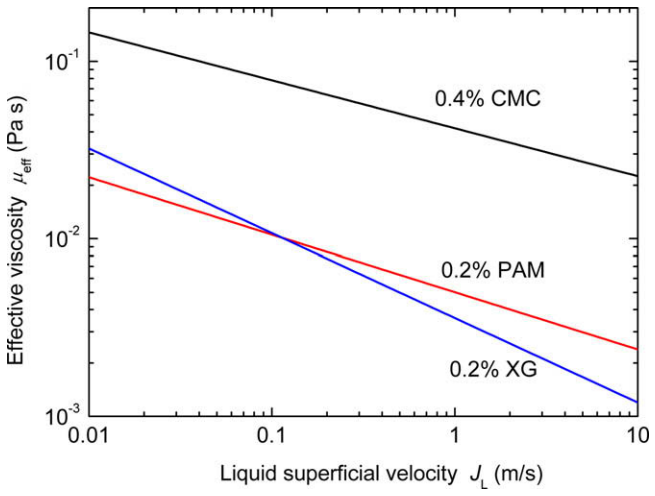

Fig. 12. Effective viscosity of the non-Newtonian fluids varies with the liquid superficial velocity.

tion, though the effective viscosities of the two solutions are close, the flow patterns and flow transitions are quite different. The reason could be attributed to the particular rheological characteristics of the solutions. An analytical model considering the real viscoelasticity should be developed to reveal the effect of the rheological properties of liquids on the flow patterns.

3.5. Comparison of flow regime maps with different channels

Fig. 14 shows the comparison of the flow regime maps for nitrogen/CMC solution two-phase flow in channels with different hydraulic diameters.

As can be found in Fig. 14 that the transition in channel T3 (D_h = 0.866 mm) from slug flow to churn flow shifts rightwards compared to that in channel T2 (D_h = 2.886 mm), which leads to a smaller slug flow region in channel T3. This may be caused by the combined effects of surface tension and channel scale. According to Table 2, the non-Newtonian fluids have nearly the same surface tension as water. However, the effect of surface tension becomes stronger for the slugs with smaller dimension (Holmber et al., 2002), which makes it possible for the slugs to remain a stable shape at higher gas superficial velocities. As the characteristic dimension of the channel decreases to the magnitude of the bubble diameter, the bubbles are much easier to be coalesced due to the viscous effect of the solution. This may explain why the dispersed bubbly (DB) flow is not found in the channel T3. The combined effect of surface tension and channel scale also leads to later transition from churn flow to annular flow for most range of liquid superficial velocity in the preset work.

Though the hydraulic diameters of channel S1 (D_h = 2.5 mm) and T2 (D_h = 2.886 mm) are close to each other, the flow pattern transitions seem to be distinguishing dramatically. Firstly, no dispersed bubbly flow is found in the channel in channel S1. Secondly, the transition from churn flow to annular flow in channel S1 occurs at a gas superficial velocity higher than that in channel T2. This indicates that the flow pattern transition is remarkably influenced by the cross-section of the channel. For channel T2, the equilateral triangular cross-section restrains the gas core more effectively,

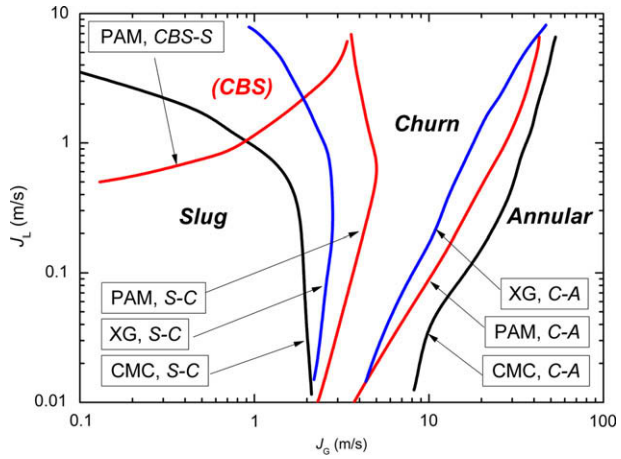

Fig. 13. Comparison of flow regime maps of different non-Newtonian fluids in test section S1.

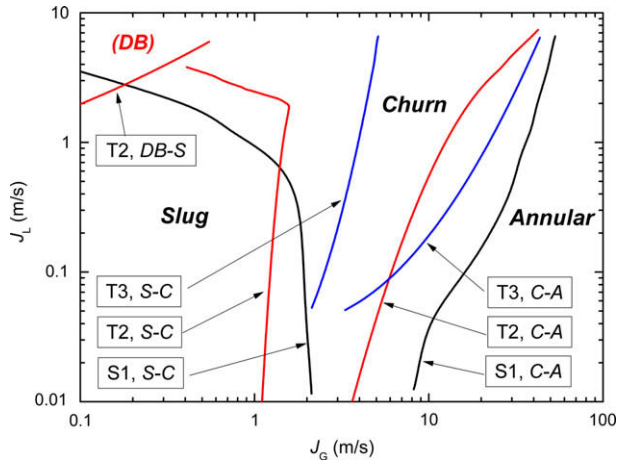

Fig. 14. Comparison of the flow regime maps for nitrogen/CMC solution in different channels.

that is, the corner region included by the walls is occupied by the liquid phase and the gas core can only flow in the center region of the channel. When more gas is added to the channel, a stable gas core is easier to be maintained, thus resulting in the transition from churn flow to annular flow occurring at lower gas superficial velocity.

3.6. Comparison with the available flow regime transitions criteria

According to Hibiki and Mishima (2001), the transition from bubble to slug flow pattern in a gap can be evaluated using the drift flux correlation

$$J_L = \frac{1}{C_0}\left[\left(\frac{1}{\alpha_{cr}} - C_0\right)J_G - J_{drift}\right] \tag{3}$$

where J_{drift} is the drift velocity of a gas bubble related to the liquid phase and its value is given by

$$J_{drift} = \sqrt{2}\left(\frac{\sigma g \Delta\rho}{\rho_L^2}\right)^{0.25}(1-\alpha_{cr})^{1.75} \tag{4}$$

and the constant C_0 in Eq. (3) is defined by

$$C_0 = 1.35 - 0.35\sqrt{\frac{\rho_G}{\rho_L}}. \tag{5}$$

In Eqs. (3)–(5), J_G and J_L are the superficial velocities of gas phase and liquid phase, respectively; ρ_G and ρ_L are the density of gas phase and liquid phase; σ, the surface tension of the liquid; the critical void fraction α_{cr} varies from 0.2 to 0.3.

As for transition from slug to churn flow, Sowinski and Dziubinski (2008) presented a transition criterion based on the work of Hibiki and Mishima (2001), i.e.,

$$\alpha_G \geqslant 0.813X^{0.75} \tag{6}$$

$$X = \frac{(C_0-1)(J_G+J_L)+J_{Drift}}{(J_G+J_L)+\gamma\left[\left(\frac{\rho_L D_h}{\mu_L}\right)^{-m}\frac{C_L\rho_L}{\Delta\rho g s}\right]^{1/(m-2)}} \tag{7}$$

in which, m and γ depend on the Reynolds number, for laminar flow $m = 1$, $\gamma = 0.15$; for turbulent flow, $m = 0.25$, $\gamma = 0.7$. C_L is a coefficient dependent on the equivalent Reynolds number of the non-Newtonian solution, defined by

$$Re' = \frac{\rho_L u D_h}{k\left(\frac{3n+1}{4n}\right)^n\left(\frac{8u}{D_h}\right)^{n-1}} \tag{8}$$

wherein, u is equal to the superficial velocity of liquid phase.

In Eq. (7), s is the channel gap. For the square channel S1, it is natural to take the side length of the channel cross-section as the channel gap, that is, $s = a$. For triangular channels, the channel gap is determined as $s = \sqrt{3}a/3$.

As for transition from churn flow to annular flow, the criterion proposed by Hibiki and Mishima (2001) is used, which is defined as

$$J_G = \sqrt{\frac{3\Delta\rho g D_h}{2\rho_G}}(\alpha_G - 0.11) \tag{9}$$

in which $\Delta\rho$ indicates the density difference between the liquid phase and gas phase.

Using Eqs. (3), (6) and (9), the flow pattern transitions can, therefore, be expressed.

Fig. 15 plots the flow regime maps of nitrogen/water, nitrogen/CMC and nitrogen/PAM in the present work. The transition criteria predicted by using Eqs. (3), (6) and (9) are also plotted. According to Fig. 15(a) and (b), it shows that even for nitrogen/water two-phase flow, Eqs. (3), (6) and (9) cannot predict the flow pattern transitions well in the present work. Moreover, Fig. 15(c) and (d) shows that the transition criteria provided by Hibiki and Mishima (2001) and Sowinski and Dziubinski (2008) have poor ability to predict the flow pattern transitions for nitrogen/non-Newtonian two-phase flow in the present work. It can be noted that for nitrogen/CMC two-phase flow in the channel T2, there is no common bubble flow but the dispersed bubble (DB) flow; and for nitrogen/PAM two-phase flow, there is special flow pattern of the chained bubble/slug (CBS) flow. However, Eq. (3) only indicates the transition of common bubble to slug flow and cannot predict the special flow patterns.

The invalidity of the transition criteria provided by Hibiki and Mishima (2001) and Sowinski and Dziubinski (2008) may be that the both models are deduced based on the water-air two-phase flow in narrow gaps. The geometrical difference of the channel and the complicated physical properties of the non-Newtonian solutions invalidate these models. This calls for more work to be carried out in order to provide feasible models for predicting the flow pattern transition criteria of gas/non-Newtonian fluids two-phase in microchannels.

4. Concluding remarks

A visualized experimental investigation on nitrogen/non-Newtonian solution two-phase flow in vertical non-circular microchan-

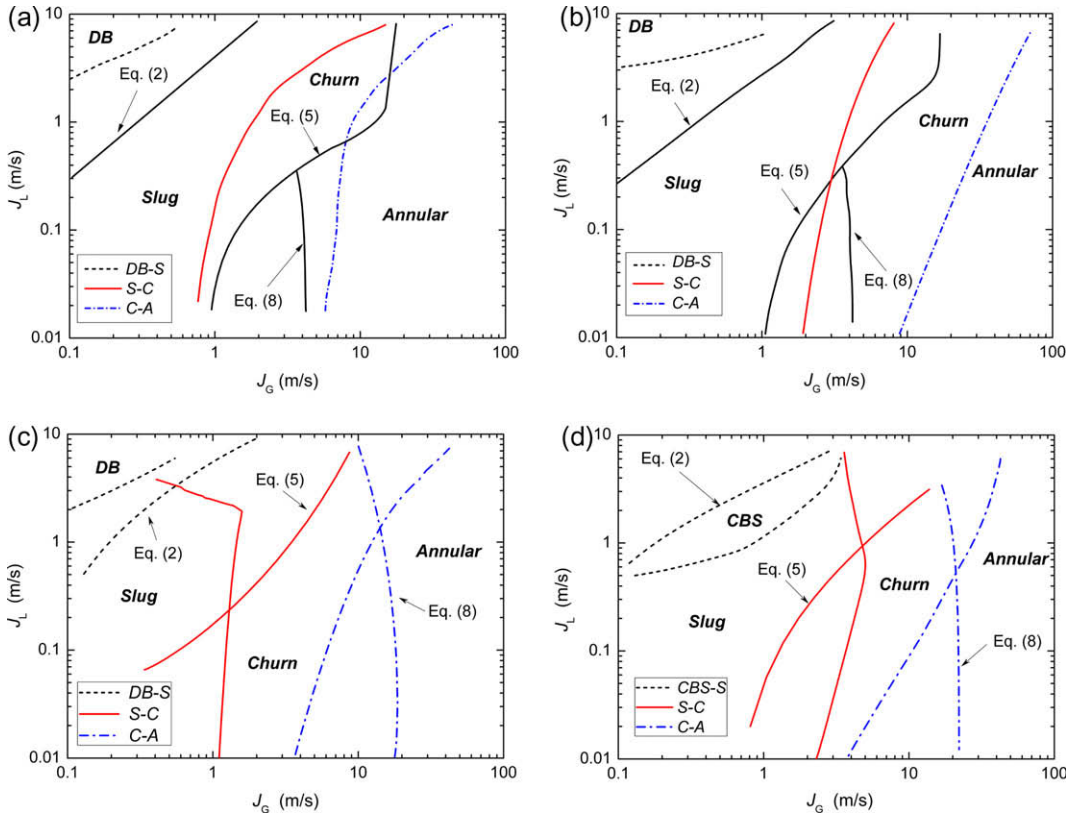

Fig. 15. Comparison with the flow regime transitions criteria by Hibiki and Mishima (2001) and Sowinski and Dziubinski (2008): (a) nitrogen/water, channel T2; (b) nitrogen/water, channel S1; (c) nitrogen/CMC solution, channel T2; (d) nitrogen/PAM solution, channel S1.

nels has been conducted. Three typical non-Newtonian solutions with different rheological characteristics, i.e., 0.4% CMC aqueous solution, 0.2% PAM aqueous solution, and 0.2% XG solution are used as the working fluids. The typical images of the nitrogen/non-Newtonian solution two-phase flow pattern are presented. And the flow regime maps for the three different working fluids have also been developed. Some concluding remarks are drawn as below.

(1) Typical flow patterns of the three different non-Newtonian solutions, i.e., slug flow, churn flow and annular flow, are observed in this work, which are similar to those had been observed in air–water two-phase flow in the channels with the same diameter. Dispersed bubbly flow has also been observed in the nitrogen/CMC two-phase flow in the channel S2 (D_h = 2.886 mm) but not found for nitrogen/CMC two-phase flow in the other two channels with smaller hydraulic diameter or for two-phase flow of the other two non-Newtonian solutions in all the test channels. A new flow pattern named chained bubble–slug (CBS) flow has been observed for nitrogen/PAM solution two-phase flow in all the channels, characterized by a chained bubble/slug flowing along the axis of the channels.

(2) It is found that the rheological properties of the non-Newtonian solution affect the flow regime transitions remarkably. The larger is the effective viscosity of the non-Newtonian fluid, the wider of the churn flow region is. The newly observed CBS flow pattern in nitrogen/PAM solution may be caused by the particular properties of non-Newtonian fluid.

(3) It is also found that the geometrical characteristics of the channel such as the hydraulic diameter and cross-section shape can influence the flow pattern transition.

(4) Comparison of the results obtained from the present work with the available flow pattern transition criteria shows a large deviation. Much more work has to be carried out for further understanding of the mechanism of gas/non-Newtonian fluid two-phase flow in the microchannels.

Acknowledgements

This work is supported by the Natural Science Foundation of China (NSFC), No. 50576076.

References

Akbar, M.K., Plummer, D.A., Ghiaasiaan, S.M., 2003. On gas–liquid two-phase flow regimes in microchannels. Int. J. Multiphase Flow 29, 855–865.
Armand, A.A., Treschev, G.G., 1946. Izv. Vses. Teplotek. Inst. 1, 16–23.
Barnes, H.A., 2000. A Handbook of Elementary Rheology. The University of Wales Institute of Non-Newtonian Fluid Mechanics, Wales.
Chen, W.L., Twu, M.C., Pan, C., 2002. Gas–liquid two-phase flow in micro-channels. Int. J. Multiphase Flow 28, 1235–1247.
Cheng, L., Ribatski, G., Thome, J.R., 2008. Two-phase flow patterns and flow-pattern maps: fundamentals and applications. Appl. Mech. Rev. 61, 050802–050828.
Cubaud, T., Ulmanella, U., Ho, C.-M., 2006. Two-phase flow in microchannels with surface modifications. Fluid Dyn. Res. 38, 772–786.
Dziubinski, M., Fidos, H., Sosno, M., 2004. The flow pattern map of a two-phase non-Newtonian liquid–gas flow in the vertical pipe. Int. J. Multiphase Flow 30, 551–563.
Hibiki, T., Mishima, K., 2001. Flow regime transition criteria for upward two-phase flow in vertical narrow rectangular channels. Nucl. Eng. Des. 203, 117–131.
Holmber, K., Jönsson, B., Kronberg, B., Lindman, B., 2002. Surfactants and Polymers in Aqueous solution. Wiley, England.
Kawahara, A., Chung, P.M.-Y., Kawaji, M., 2002. Investigation of two-phase flow pattern, void fraction and pressure drop in microchannel. Int. J. Multiphase Flow 28, 1411–1435.
Mandhane, J.M., Gregory, G.A., Aziz, K., 1974. A flow pattern map for gas–liquid flow in horizontal pipes. Int. J. Multiphase Flow 1, 537–553.

Saisorn, S., Wongwises, S., 2008. Flow pattern, void fraction and pressure drop of two-phase air–water flow in a horizontal circular microchannel. Exp. Therm. Fluid Sci. 32, 748–760.

Serizawa, A., Feng, Z., Kawara, Z., 2002. Two-phase flow in microchannels. Exp. Therm. Fluid Sci. 26, 703–714.

Sowinski, F.J., Dziubinski, M., 2008. Experimental study on gas–viscous liquid mixture flow regimes and transitions criteria in vertical narrow rectangular channels. Proc. World Acad. Sci. Tech. 30, 618–621.

Spisak, W., 1986. Two-phase flow of gas–highly viscous liquid. Wroclaw Technical University, Poland.

Triplett, K.A., Ghiaasiaan, S.M., Abdel-Khalik, S.I., Sadowski, D.L., 1999. Gas–liquid two-phase flow in microchannels, Part I: two-phase flow patterns. Int. J. Multiphase Flow 25, 377–394.

Wu, Q.Y., Wu, J.A., 2002. Rheology of Polymer Materials. Higher Education Press, Beijing.

Xu, J.L., Cheng, P., Zhao, T.S., 1999. Gas–liquid two-phase flow regimes in rectangular channels with mini/micro gaps. Int. J. Multiphase Flow 25, 411–432.

Xu, J., Wu, Y., Shi, Z., Lao, L., Li, D., 2007. Studies on two-phase co-current air/non-Newtonian shear-thinning fluid flows in inclined smooth pipes. Int. J. Multiphase Flow 33, 948–969.

Zhao, T.S., Bi, Q.C., 2001. Co-current air–water two-phase flow patterns in vertical triangular microchannels. Int. J. Multiphase Flow 27, 756–782.